Adv. Space Res. Vol. 8, No. 1, pp. (1)279–(1)289, 1988
Printed in Great Britain.

0273–1177/88 $0.00 + .50

VLF WAVE-INJECTION EXPERIMENTS FROM SIPLE STATION, ANTARCTICA

R. A. Helliwell

Space, Telecommunications and Radioscience Laboratory, Stanford University, Stanford, CA 94305, U.S.A.

ABSTRACT

The background of VLF wave-particle experiments from Siple Station, Antarctica, is briefly reviewed. Most of these results are interpreted in terms of Doppler shifted cyclotron interaction between energetic electrons and the VLF waves near the equatorial plane. Single frequency ducted signals that exceed a certain 'threshold' intensity are observed at the conjugate point (Roberval, or Lake Mistissini, Quebec) to be amplified 30-50 dB, with temporal growth rates of 30-200 dB/s. Following saturation, variable frequency emissions are triggered. With the addition of a second signal, separated in frequency from the first by $\Delta f < 100$ Hz, signal growth at both frequencies is reduced and sidebands are generated at frequencies separated from the carriers by integer multiples (up to seven) of Δf. The sidebands are attributed to short emissions triggered by the beats between the two input carriers. Midlatitude magnetospheric hiss is crudely simulated by a sequence of 10 ms pulses whose frequencies are chosen randomly within a 400 Hz band. Results show that certain combinations of 10 ms pulses link together to form chorus-like elements, suggesting a common origin for hiss and chorus. In contrast to the equatorial region phenomena are low altitude (1000-8000 km) satellite observations of narrowband Siple pulses showing increases in bandwidth of up to 1000 Hz with impulsive triggered emissions of similar bandwidth; these phenomena are interpreted in terms of a new type of quasi-electrostatic plasma instability in the subauroral region of the magnetosphere, involving 200 m wide field aligned irregularities and occurring at frequencies near the lower hybrid resonance frequency. A new crossed dipole antenna at Siple Station that generates left-hand, right-hand, or linear polarization is used to increase the effective radiated power and to perform polarization experiments.

INTRODUCTION

Experiments are described in which very low frequency waves are injected into the magnetosphere from Siple Station, Antarctica. The signals are observed on various satellites within the magnetosphere and at a conjugate station located at Lake Mistissini, Quebec. The aim of these experiments is to understand the propagation of VLF waves in the ionosphere and magnetosphere and their interactions with energetic charged particles. There are two major topics of interest. The first, which is the subject of this paper, is the growth, saturation, and triggering of VLF waves due to the interaction between coherent input waves and energetic charged particles. The second is wave-induced particle precipitation and its effects on the ionosphere. Observation of wave-induced particle precipitation provides new information on the nature of the earth's radiation belts and the generation of aurora, x-rays, and the enhancement of the thermal ionization in the ionosphere. Such enhancements can affect propagation over a wide frequency range, from 2.5 kHz to 900 kHz. Wave-induced particle precipitation effects have already been observed in association with strong radio signals transmitted from stations NAA and NSS and whistlers excited by atmospheric lightning /1/.

A remarkable property of VLF wave growth and triggering is their dependence on coherence of the input signal. Strong wave growth is observed only when the bandwidth of the input signal is less than roughly 10 Hz. Because of this fact the phenomenon has been termed the coherent wave instability (CWI). One of the purposes of the experiments is to explore the CWI, which appears to be present at Jupiter, Saturn and Uranus, and to thereby advance our understanding of nonlinear plasma physics. The general nature of the experiments to be discussed in this paper is illustrated in Figure 1 which shows a duct of slightly enhanced thermal ionization that serves to trap the VLF waves injected from Siple Station. Near the equatorial plane it is hypothesized that these waves interact with doppler-shifted cyclotron resonant electrons to create new waves that increase the intensity of the output signal and generate new signals called VLF emissions. These amplified signals and associated emissions scatter resonant electrons from the radiation belts into the ionosphere where they convert their energy to other forms. Several ducts may be excited simultaneously; as many as 30 ducted whistlers have been observed from one lightning discharge. Several ducts may simultaneously show amplifying effects thereby extending the area affected by wave-induced precipitation. In Figure 1 the received signal in part (f) shows two similar emissions that are attributed to propagation and triggering in two separate ducts.

SINGLE FREQUENCY EXPERIMENTS

Because of the importance of coherence, we first review the results of single frequency experiments from Siple Station. A typical case of wave growth and saturation is shown in Figure 2. A one-second pulse at 2000 Hz grows exponentially with time; following saturation a band limited impulse (BLI) and a rising emission are triggered. A key feature of the growth process is the smooth increase in signal phase with time /3/. Neither phase advance nor saturation have yet been satisfactorily explained theoretically.

In addition to exponential growth, saturation and triggering, the CWI is characterized by a well defined threshold. An example is shown in Figure 3 in which a 3-s long transmitted pulse was slowly increased in amplitude as shown by the solid line in the middle panel. At first the output signal follows the input signal except for the 8 Hz beat with a harmonic from the Canadian power system. Near the middle of the pulse, within 2 dB of the maximum amplitude of the input signal, the received intensity shows a sudden increase in slope, to about 90 dB/s. This effect is known as the growth threshold and has been found to vary widely with time, as much as 20 dB over a period of several minutes /4/. Of particular interest is the phase behavior, as shown in the lower panel. As the signal intensity at the input is increased we see that the phase is essentially constant. The significant point is that there is no change in phase until the growth threshold is reached. Then the phase advances monotonically with time, except for small glitches due to atmospherics, until saturation is reached. We conclude therefore that the phase advance cannot be simply explained by some transient effect associated with the onset of the input signal. Rather it appears that the phase begins to advance when temporal growth begins. Following triggering the carrier intensity drops briefly to a value below the applied signal. This effect has not been explained but suggests the possibility that the carrier is attenuated by the triggered riser acting on the phase bunching process in such a way as to create a stimulated signal that is temporarily out of phase with the applied signal. Following this brief period of reduced intensity the carrier is again amplified at the same rate as before, reaches the same saturation level and triggers a similar kind of emission. A third emission is generated before the applied pulse ends. The phenomena of Figures 2 and 3 together constitute a definition of the principle features of the CWI as it applies to single frequency wave growth and triggering in the magnetosphere.

TWO-FREQUENCY EXPERIMENTS

When two or more coherent wave signals with frequency separations less than about 100 Hz are injected into the magnetosphere, an entirely new class of phenomena is observed. First we should note that for frequency separations exceeding $\sim$ 100 Hz, the input waves behave essentially like single frequency signals whose properties are illustrated in Figures 2 and 3. However, for frequency separations less than 100 Hz very different effects are observed. We illustrate these effects for the case of two frequencies spaced 20 Hz apart, as shown in Figure 4. In the period between 6 and 7 seconds there are two equal-amplitude waves spaced 20 Hz apart, showing predictable beating in the received signal (middle and top panels) at the 20 Hz rate. It is clear that there is no significant temporal growth of these two signals until the lower signal is turned off. At that instant the upper frequency component begins to grow at a typical exponential rate. Saturation and triggering follow just as in the case of the single frequency pulses shown in Figures 2 and 3. This result is confirmed by the onset of a single frequency signal in the left-hand part of the diagram between analog tape.) 3 and 4 seconds. There the growth rate is approximately the same as that after recovery in the 7 to 8 s portion of the record, with peak amplitudes being roughly the same. Differences in the shapes of the growth curve are attributed to multi-path propagation which is present in most of these experiments and which alters the envelope in a manner that depends on the relative phasees of the component signals. The important conclusion from Figure 4 is that closely spaced coherent waves suppress the growth of one another. Furthermore, when one of the two signals is turned off the exponential growth of the remaining signal begins immediately. Thus there is no delay in suppression as has been suggested in connection with the so-called quiet band effect /5/ /6/.

A variation of the experiment of Figure 4 is obtained by ramping the amplitude of one of the two components up and down. In Figure 5 we show the results of a +20 dB/s ramp of the lower component in the interval 3 to 4 s and a corresponding -20 dB/s ramp in the interval 7 to 8 s. The resulting change in the spectrum is quite remarkable. In the left-hand up-ramp segment the upper signal first begins to grow at the expected single frequency rate, but at a ramp level of ~ -15 dB the weak lower signal creates strong sidebands over a relatively wide range of frequencies. In the right-hand portion of the diagram the reverse effect is seen as the lower frequency signal is reduced in amplitude. However there is a little delay in the development of the sidebands in this case because the upper signal must grow from a fully suppressed level before it can generate sidebands. Experiments of this kind have shown sidebands with orders as high as 7 and significant sideband components in the range $10 < \Delta f < 100$ Hz. At times the sideband intensities can exceed the carrier levels and on occasion the carriers themselves have been suppressed by the sidebands. An explanation of sideband generation has been suggested as follows /7/. Each beat acts like an independent amplitude modulated signal at $f = (f_1 + f_2)/2$, which triggers an initially rising emission. This emission is entrained or cut off by the next emission and the process repeats. The result is a series

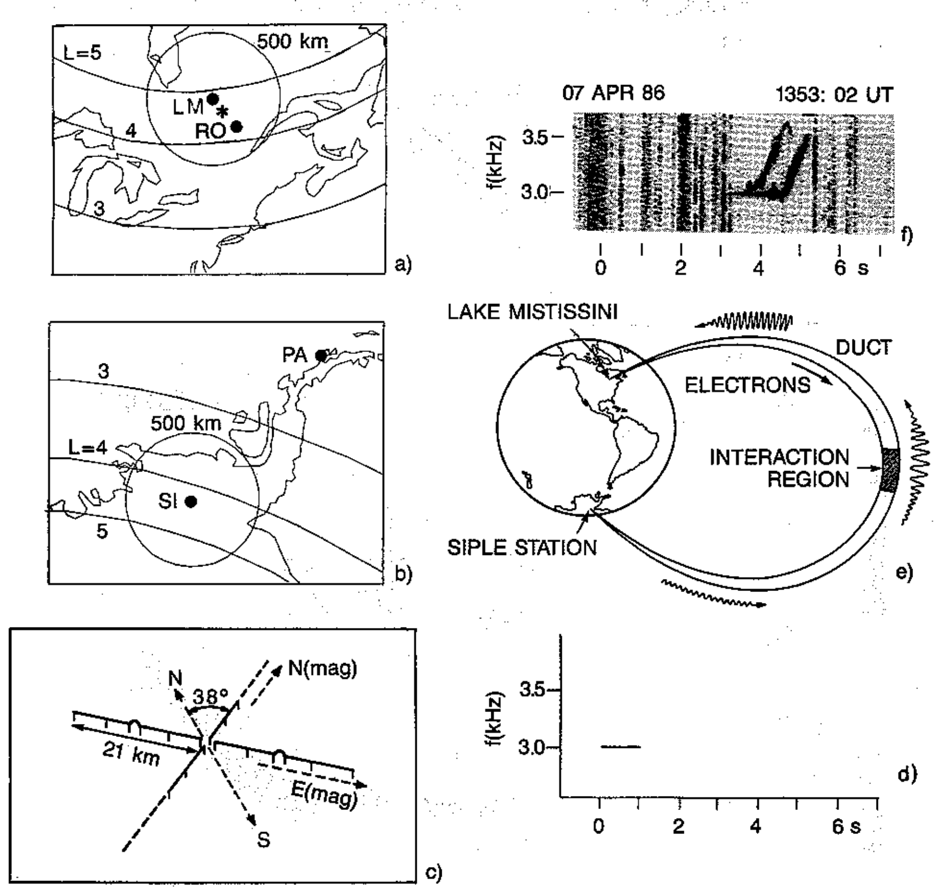

Fig. 1. Siple/Lake Mistissini experiment plan. (a) map showing the new station, Lake Mistissini (LM), previous station, Roberval (RO), and estimated Siple Station conjugate point (*) for 1986 /2/. (b) Map of Antarctic peninsula, showing Siple Station (SI) and Palmer Station (PA). (c) Crossed dipole antenna at Siple, with planned extensions shown as dashed lines. (d) f–t diagram of one-sec pulse at 3 kHz. (e) Diagram of duct propagation path from Siple to conjugate region, showing wave growth near equatorial plane. (f) f–t diagram of two one-hop amplified signals with associated emissions that propagated to LM in two ducts that were excited by the one sec pulse of (d).

of short pulses that are similar in shape and are modulated in frequency and amplitude, giving rise to a sideband spectrum that can have considerable variation in its frequency content and furthermore can have unsymmetrical upper and lower sidebands, as suggested by the results of Figure 5. It is important to note that the maximum sideband output in Figure 5 occurs when the ratio of the two input signals is $\sim$ 12 to 15 dB. On the other hand strong sidebands have been observed to occur at other times when the two signals were equal in strength. This means that any strong coherent signal in the magnetosphere is likely to beat with other weaker signals such as echos of previous signals, whistlers, chorus, or power line harmonics. One should expect therefore that the normal behavior of the magnetosphere is to generate many new components as a result of the interaction of two or more coherent signals with spacing in the range 10 to 100 Hz. Thus the injection of coherent waves leads naturally to a broadening of the spectrum and a reduction in the coherence of the overall output. This process might therefore play a role in the generation of various kinds of noise-like natural signals such as midlatitude hiss.

NOISE SIMULATION EXPERIMENTS

The results of the two frequency experiments described in Section C suggest that it may be possible to explain hiss on the basis of interactions between quasi-coherent input signals. Such speculation leads naturally to the idea that the natural hiss might be simulated by the Siple transmitter. Such an experiment is illustrated in Figure 6 /8/. Here an approximation to magnetospheric hiss is created by frequency

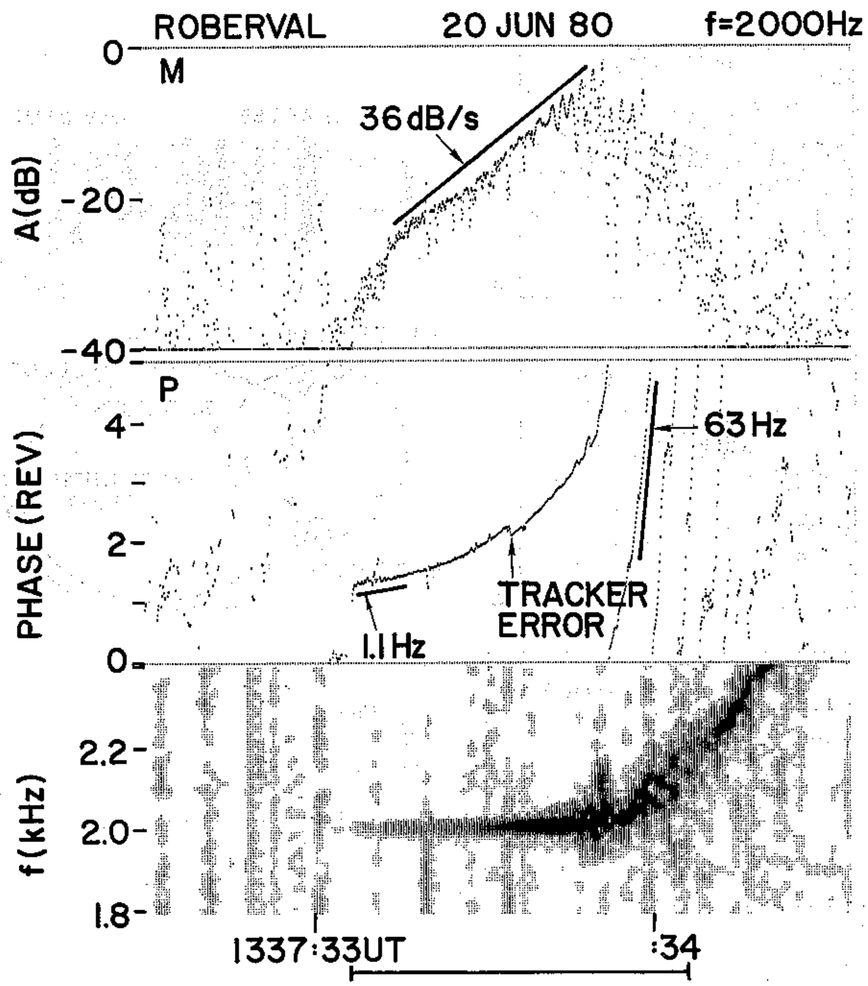

Fig. 2. Digital analysis of dynamic spectrum (bottom panel), phase track (middle panel) and amplitude in dB of a one-hop pulse injected from Siple Station at 2 kHz. Transmitted one-sec pulse corrected for path delay is shown at bottom.

modulating a constant amplitude carrier. The modulation consists of changing the frequency every 10 ms within a band 400 Hz wide using a table of random numbers to choose the frequencies. This sequence of random frequencies is repeated once each second and the resulting spectrum as transmitted from Siple Station is shown in the upper part of Figure 6. The signals as received at the conjugate point in Roberval, Canada are shown in parts b and c. Here the 1-s periodicity is quite clear but it is also noted that the spectral shapes change slowly with time. In panel b we see chorus-like elements which form out of the background of the relatively random hiss elements. These chorus elements clearly repeat at the one-sec repetition rate. However 20-s later, in panel c, where the same format is transmitted, we see little evidence of the previous chorus elements. These observations suggest that when the phasing is favorable a series of relatively independent wavetrains can link together to create a pseudo coherent wavetrain. These short wavetrains, lasting about 100-200 ms, in fact do resemble the elements of magnetospheric chorus.

To demonstrate the similarity of the received spectra to random noise we show in panel d a spectrum of white noise using the same analyzer and in section e an example of natural hiss from the magnetosphere. The reason that panels b and c resemble the white noise more than they resemble the transmitted spectrum in panel a is that dispersion along the path shifts the relative times of arrival of the transmitted 10 ms wavetrains causing them to interfere with one another and create a noise-like amplitude spectrum. This is why the frequency modulation format employed in this experiment produces a received spectrum that resembles band-limited white noise. It has the advantage that the peak power output from the transmitter can be employed whereas an actual simulation by the transmitter of random noise would require a considerable reduction in the average power in order to accommodate the peaks of the noise.

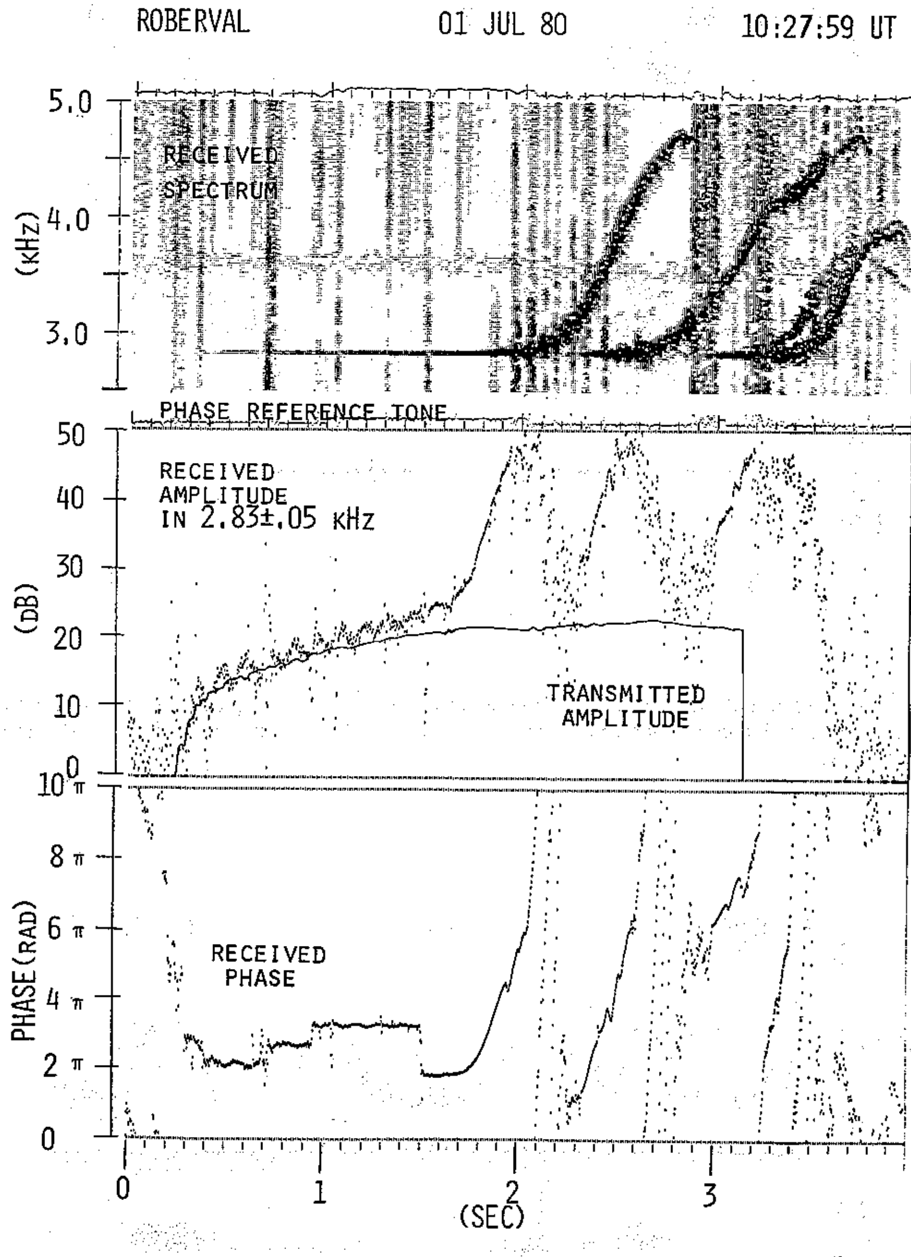

Fig. 3. Digital analysis of 3-sec long pulse showing threshold effect for growth and triggering. (a) Dynamic spectrum. (b) Amplitude versus time of received signal (shown by dots) within a 100-Hz band centered at transmitter frequency. Amplitude of transmitted signal is ramped up with time as shown by solid line. (c) Received phase showing onset of phase advance close to time of fast temporal growth. The earlier phase jumps were caused by sferics appearing in panel (a).

A further test of the similarity of the simulated noise to that observed naturally is shown in Figure 7 where risers are triggered at the top edge of the simulated noise band, a feature often seen in the case of natural phenomena.

Comparing the results of Figures 5 and 6 we recognize two opposite processes. In Figure 5 we see evidence of coherent waves being reduced to noisy structures consisting of complicated systems of sidebands. In Figure 6 we see the reverse process in which irregular wavetrains link together to form simpler, more coherent wavetrains. If we put these two pictures together and assume an adequate amount of echoing over the path, we have a basis for an equilibrium model. In this model chorus-like elements are continually being generated by the process demonstrated in Figure 6, whereas noise is continually being generated by

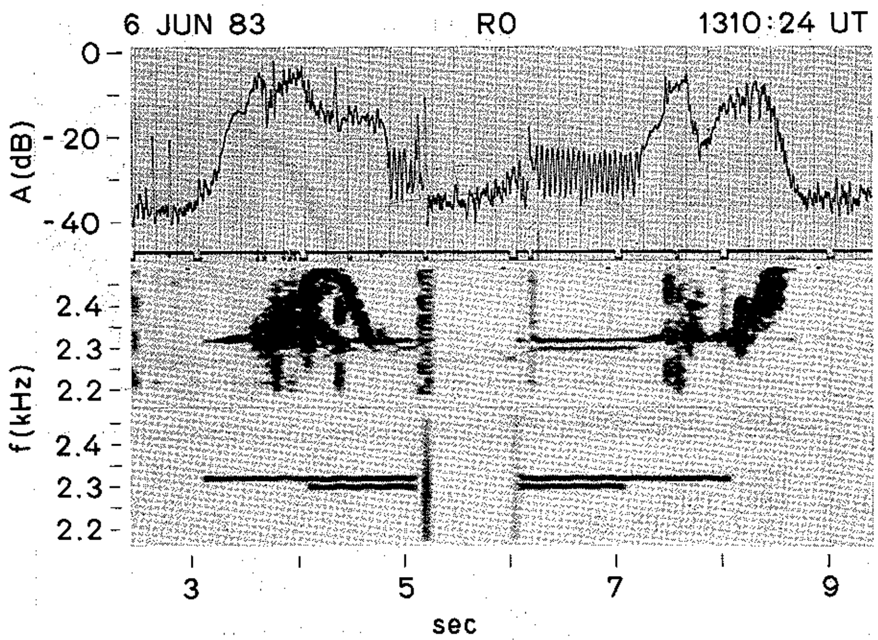

Fig. 4. Single and double ($\Delta f = 20$ Hz) frequency response. Bottom panel shows transmitted format; middle panel, signals received at Roberval; top panel, total intensity of received signals in 300 Hz band.

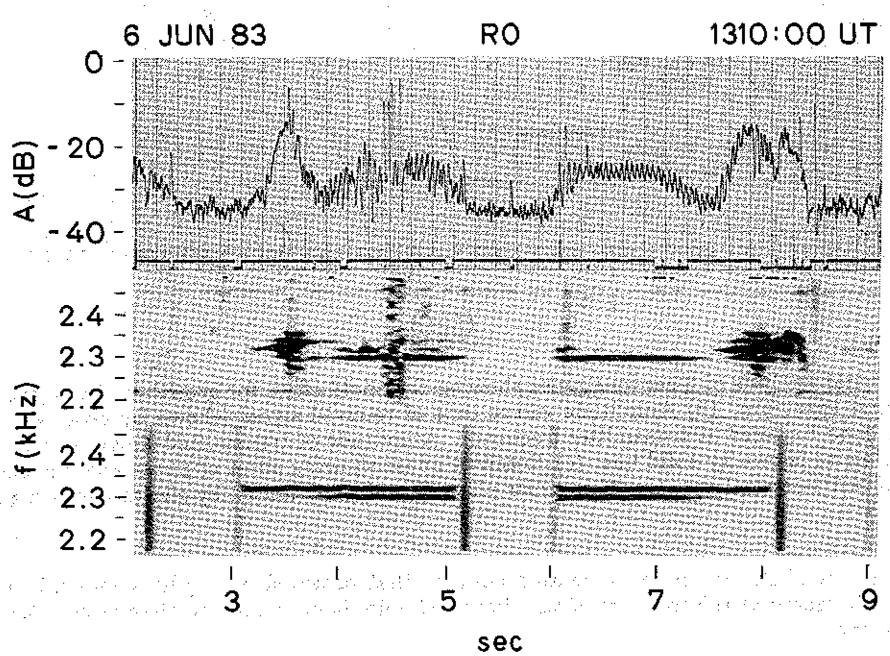

Fig. 5. Same as Figure 4, except lower frequency component ramped in amplitude at rates of +20 dB/s in 3 to 4 sec period and at -20 dB/s in 7 to 8 sec period. Transmitted format is aligned in time with principal received component.

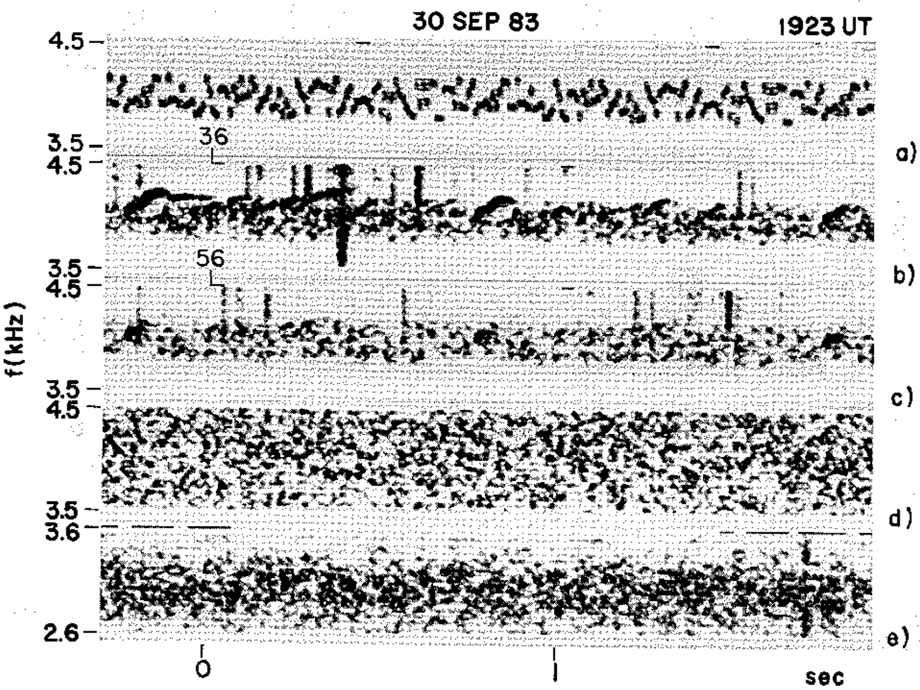

Fig. 6. Hiss spectra for 20-Hz filter bandwidth. (a) Transmitted spectrum, with 1-s periodicity. (b) and (c) Received spectra taken 20 s apart showing changes and similarities in 1-s pattern. (d) Spectrum of hiss from a laboratory random noise generator. (e) Spectrum of natural hiss received at Roberval on February 14, 1977 at 1216 UT.

the process illustrated in Figure 5. If these two processes were to occur simultaneously the result would be a combination of hiss and chorus, each one creating some of the other. This description is suggestive of the properties of mid-latitude hiss (See Figure 6e). Further experiments will be required in order to test this hypothesis and to identify and measure the parameters which control the process. It is suggested that the critical factors are the reflection coefficients at the ends of the echoing path, the threshold for temporal growth as defined in Figure 3, the growth rate, and the suppression of adjacent signal growth as defined in Figure 4. Since growth rate is known to vary with frequency one can see that the banded character of most hiss and chorus would be naturally related to the growth rate as defined by Figure 2.

SPECTRAL BROADENING

With the aid of satellites such as EXOS-B, DE-1, ISEE-1, and ISIS-2 we observe the properties of nonducted Siple signals which cannot be detected on the ground. It has been discovered, for example, that Siple signals seldom trigger emissions in the nonducted mode. However it has also been observed that amplification and triggering that occurs inside of ducts as shown in Figures 2 and 3 produces signals that reflect back from the lower edge of the ionosphere into the magnetosphere in the nonducted mode where they can be readily observed by satellites. This so-called "hybrid" mode couples the ducted and nonducted modes together and provides a mechanism by which amplified signals and emissions from ducts can be observed in other parts of the magnetosphere /9/.

At lower altitudes another relatively new effect called spectral broadening has been discovered. This is illustrated in Figure 8 which shows a Siple signal format as observed on the ISIS satellite at 1400 km altitude. The significant effect is the broadening of the Siple spectrum when the frequency is above the local hybrid resonance frequency. Such broadening effects have been observed to cover a band as wide as 1 kHz and have been seen in connection with virtually all VLF waves injected from the ground and observed on satellites. In addition, emissions in the form of band-limited impulses of $\sim$ 20 ms duration and a bandwidth of $<$ 1 kHz have been found to occur in connection with the Siple signals as shown in the figure. This process of impulsive emission triggering appears to be related to particle precipitation which produces ionospheric irregularities that may in turn be responsible for spectral broadening. These impulsive emissions are

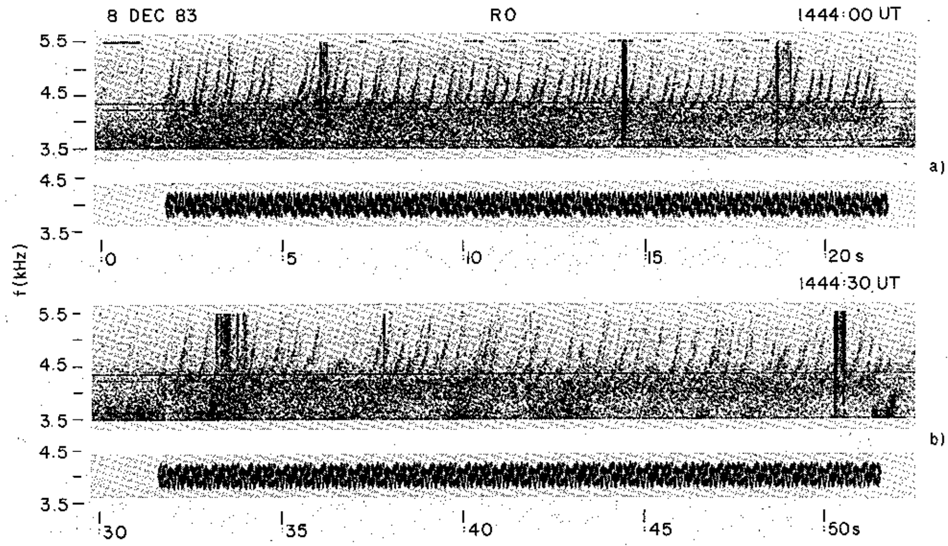

Fig. 7. (a) 400-Hz hiss band triggers chorus with pronounced 1-s periodicity. (b) Same, but with inverted sequence of element frequencies.

thought to be connected with rapidly evolving quasi-electrostatic emissions triggered by the Siple pulses /10/. The free energy for this process would be supplied by the precipitating energetic electrons. On the other hand the more continuous spectral broadening described above is thought to be a passive process in which the upgoing waves are scattered by ionospheric irregularities into directions close to the resonance cone. This causes the wavelength to be greatly reduced and the travelling satellite therefore sees a doppler shifted wave frequency, either up or down, that is relatively large, on the order of several hundred Hz. On the other hand such effects, although passive in nature, appear to be associated with the precipitation effect which gives rise to the irregularities that cause the scattering. The associated impulsive emissions, which may involve an active wave instability, appear to be quite different from that associated with the cyclotron interaction near the equatorial plane. The Siple transmitter is ideally suited to study this important new type of wave-particle interaction occurring in the lower regions of the magnetosphere.

POLARIZATION EXPERIMENTS

From the saturation and threshold effects, it is clear that higher effective radiated powers are needed in order to explore fully the nonlinear properties of the coherent wave instability. As a relatively inexpensive way of getting more power from the Siple transmitter a circularly-polarized crossed dipole has been erected. Its purpose is to provide for the radiation of a right-hand circularly polarized wave which is predicted to increase the amount of transmitter energy that can be coupled into the whistler mode. For overhead injection it is estimated on the basis of classical magneto-ionic theory /11/ that right circular polarization will double the effective radiated power of the transmitter. Preliminary results of this modification to the Siple wave-injection experiments are shown in Figure 9. With right-hand polarization the initial value of the received signal is +18 dB and for left-hand polarization the initial value of the received signal is +6 dB. For the left-hand case there is no temporal growth and no emission triggering so there is no significant change in the intensity with time. However for right-hand polarization the growth threshold (see Figure 3) is exceeded and we see the expected temporal growth and triggering of emissions. The peak value of the signal is +35 dB or a total increase of 29 dB with respect to the left-hand polarized wave.

There are two important effects occurring here. First the injected RH wave is greater in intensity as is expected from theory. In this case the increase is $\sim$ 12 dB suggesting that the entrance point to the duct was close enough to Siple Station to put most of the energy into the RH mode. However for highly oblique signals from Siple Station the transmitted circularly polarized wave will be projected onto the interface boundary at a relatively high angle causing the projected polarization to be eliptical instead of circular. When this projected ellipse is resolved into right- and left-hand components, a significant amount of right-hand polarization energy is excited by a left-hand polarized signal. Thus a significant response to left-handed polarization can, in the absence of any other information on the location of the duct end points, be ascribed to off-vertical penetration of the ionosphere. The other important factor is

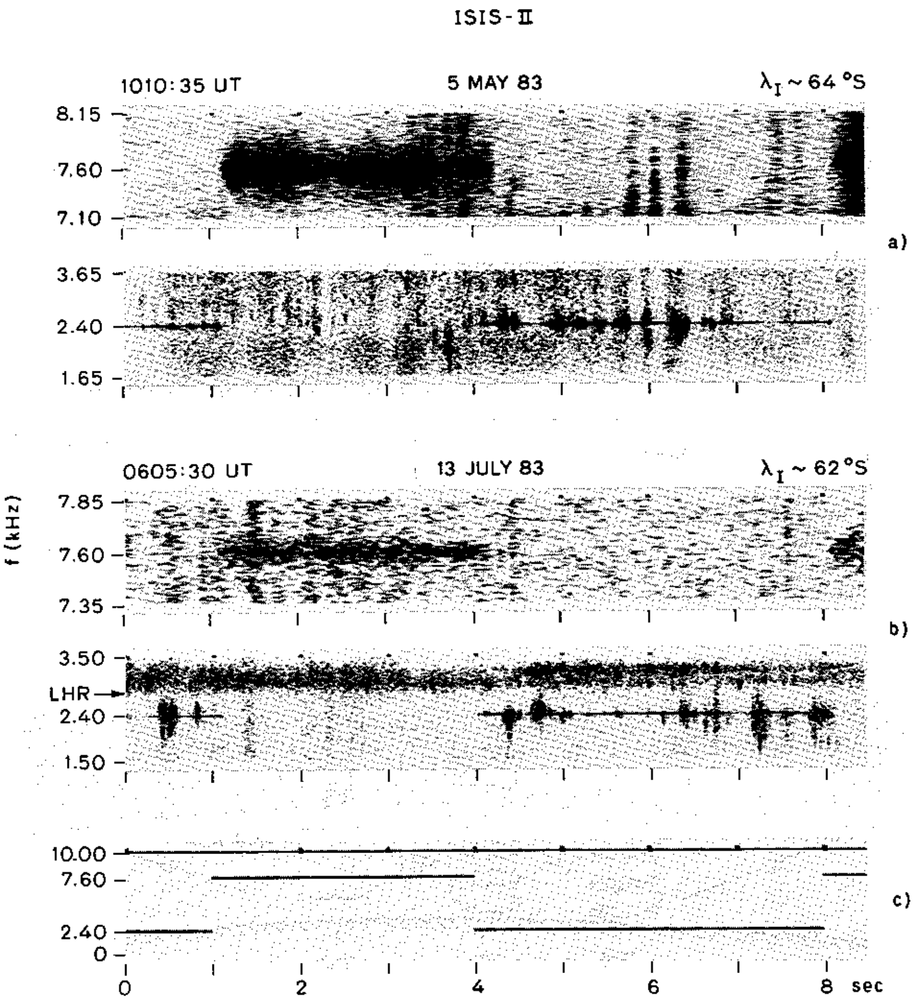

Fig. 8. High time resolution spectrograms showing the association between the spectral broadening exhibited by transmitter pulses at 7.6 kHz and impulsive VLF emissions triggered by pulses at 2.4 kHz.

the threshold effect. With the higher radiated power of the circularly polarized antenna, more independent paths can be raised above threshold, thus increasing the rms field intensity at the receiver. Preliminary observations indicate that on occasion the advantage of right-hand polarization over the previous linear polarization could be as much as 10 dB, in terms of total received signal power. Thus for experiments involving precipitation into the ionosphere from several ducts close to the transmitter, it appears that it may be possible to obtain as much as a 10 dB increase in effective precipitation.

In addition to its power gain as described above, the crossed dipole array provides a basis for new types of polarization experiments. One is to investigate the possiblity that the ionosphere is not isotropic in its physical properties. Thus field aligned irregularities might have the effect of scattering left-hand circularly polarized waves into the right-hand mode. Thus it is possible that the classical homogeneous model that is commonly used may not be correct. To be effective, such experiments would need to be conducted using direction finding techniques to determine the location of the ducts. Another class of experiments that is accessible to current techniques is the study of propagation in the earth-ionosphere waveguide. With the new crossed antenna, an effective dipole oriented in any desired direction can be created. Thus one can generate signals that are polarized in the plane of propagation or perpendicular thereto, or a combination thereof. Since pronounced differences have been found in the propagation of subionospheric waves to Palmer and Halley Bay, this experiment is likely to yield valuable new information on the response of the ionosphere to different incident polarizations.

By reciprocity the results of the experiment shown in Figure 9 can be extrapolated to the receiving case. Thus a receiver equipped with left-hand and right-hand polarized loop antennas could discriminate against magnetospheric noise components in favor of linearly polarized signals, travelling in the earth-ionosphere

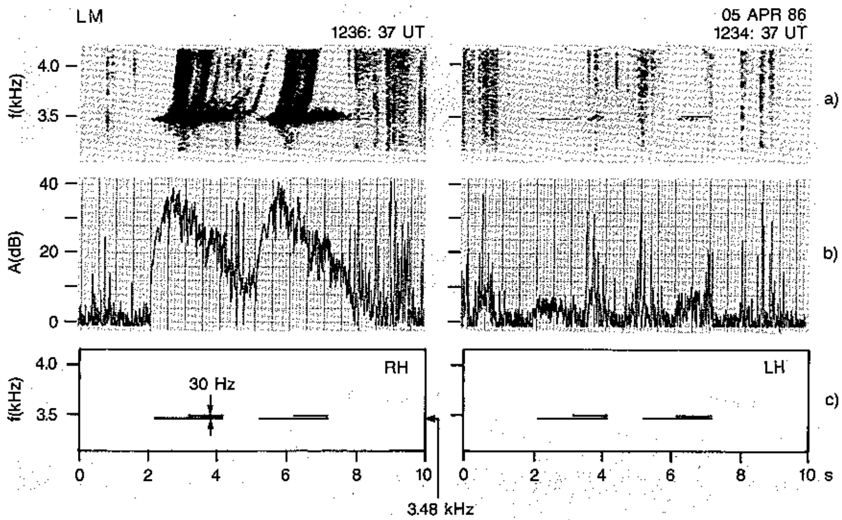

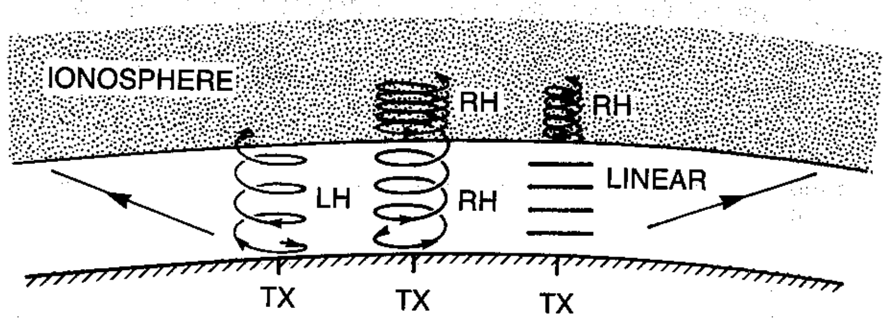

Fig. 9. Example of polarization experiment. (a) Spectra of response to right-hand (RH) (left side of figure) and left-hand (LH) transmitted polarizations. (b) Amplitude of above in 300 Hz filter centered on transmitted frequency at 3.48 kHz. (c) Transmitted format. (d) Schematic of excitation by different polarizations.

waveguide. For high latitude stations, where strong magnetospheric emissions are frequently present, such discrimination could produce significant increases in signal to noise ratios. A further application of the reciprocal experiment would be in the identification of overhead signals emanating from the ionosphere. In this case one would assume that the downcoming magnetospheric waves are right-hand circularly polarized. However the same effect mentioned above, namely the scattering by ionospheric field aligned irregularities, could create left-hand polarization from an incident right-hand wave coming down from above. Thus the study of the received signals in conjunction with direction of arrival measurements could when combined with the transmitter experiments, provide interesting new experimental opportunities for studying irregularities in the ionosphere.

As a final comment on the possible development of antenna arrays we should note that further increases in effective radiated power could be achieved by using arrays of crossed dipoles. The losses in the Antarctic ice sheet, although relatively low compared with ordinary ground, are sufficiently high that the antennas are essentially uncoupled when their parallel elements are separated by 10 kilometers or more. The reason is that antenna elements close to the ice see mainly the losses in the local portion of the ice sheet; the coupled impedance from adjacent antennas is then not very important. In this circumstance the antennas in an array can be put much closer together than would be appropriate for a free space array. It is estimated that an array of four crossed dipoles could increase the upward radiated power by a factor of four with respect to the present cross.

CONCLUSIONS

The Siple wave-injection facility has led to many new VLF wave phenomena and has been shown to be capable of duplicating most of the known natural VLF phenomena in the magnetosphere with the exception of wave-induced particle precipitation effects in the lower ionosphere. The increase in effective radiated power obtained with the crossed dipole as discussed above increases the probability that detectable wave-induced particle precipitation can be achieved in the near future. The finding that midlatitude hiss can be simulated with the transmitter enlarges the scope of studies of nonlinear coherent wave effects in the magnetosphere. Thus magnetospheric hiss joins chorus and discrete emissions as objects of quantitative controlled experimentation from the ground.

ACKNOWLEDGEMENTS

The work of J. P. Katsufrakis in managing the Stanford VLF field program and evaluating incoming data, and the efforts of field engineers D. Shafer, J. Logan, M. Dermedziew, J. Billey, and J. Green are gratefully acknowledged. Spectrograms were prepared by J. Yarbrough, and the typscript by G. Walker. Support for this research was provided by the Division of Polar Programs of the National Science Foundation under grants DPP83-17092 and DPP83-18508.

REFERENCES

1. U. S. Inan, D. L. Carpenter, R. A. Helliwell, and J. P. Katsufrakis, Subionospheric VLF/LF phase perturbations produced by lightning-whistler induced particle precipitation, *J. Geophys. Res., 90,* 7457 (1985a).

2. E. G. Stassinopoulos, L. J. Lanzerotti, and T. J. Rosenberg, Temporal variations in the Siple Station conjugate area, *J. Geophys. Res., 89*, 5655 (1984).

3. E. W. Paschal, and R. A. Helliwell, Phase measurements of whistler mode signals from the Siple VLF transmitter, *J. Geophys. Res., 89*, 1667 (1984).

4. R. A. Helliwell, D. L. Carpenter, and T. R. Miller, Power threshold for growth of coherent VLF signals in the magnetosphere, *J. Geophys. Res., 85*, 3360 (1980b).

5. R. Raghuram, T. F. Bell, R. A. Helliwell, and J. P. Katsufrakis, Quiet band produced by VLF transmitter signals in the magnetosphere, *Geophys. Res. Lett., 4*, 199 (1977).

6. N. Cornilleau-Wehrlin, and R. Gendrin, VLF transmitter-induced quiet bands: a quantitative interpretation, *J. Geophys. Res., 84*, 882 (1979).

7. R. A. Helliwell, U. S. Inan, J. P. Katsufrakis, D. L. Carpenter, Beat excitation of whistler mode sidebands using the Siple VLF transmitter, *J. Geophys. Res., 91*, 143 (1986a).

8. R. A. Helliwell, D. L. Carpenter, U. S. Inan, J. P. Katsufrakis, Generation of band limited VLF noise using the Siple transmitter: a model for magnetospheric hiss, *J. Geophys. Res., 91*, 4381 (1986b).

9. K. Rastani, U. S. Inan, and R. A. Helliwell, DE-1 observations of Siple transmitter signals and associated sidebands, *J. Geophys. Res., 90,* 4128 (1985).

10. T. F. Bell, J. P. Katsufrakis, and H. G. James, A new type of VLF emission triggered at low altitude in the subauroral region by Siple Station VLF transmitter signals, *J. Geophys. Res., 90*, 183 (1985).

11. K. G. Budden, *The Propagation of Radio Waves*, Cambridge University Press, 1985.